B142+: A magic number double-ring cluster

Yuan Yuan and Longjiu Cheng

Citation: J. Chem. Phys. **137**, 044308 (2012); doi: 10.1063/1.4738957
View online: http://dx.doi.org/10.1063/1.4738957
View Table of Contents: http://jcp.aip.org/resource/1/JCPSA6/v137/i4
Published by the American Institute of Physics.

B_{14}^{2+}: A magic number double-ring cluster

Yuan Yuan (袁媛) and Longjiu Cheng (程龙玖)[a)]
School of Chemistry and Chemical Engineering, Anhui University, Hefei, Anhui 230039, China

(Received 7 May 2012; accepted 10 July 2012; published online 27 July 2012)

B_{20} is a "magic number" cluster with double-ring structure. Surprisingly, we also find that B_{14}^{2+} is a "magic number" cluster with double-ring structure, which has the largest HOMO-LUMO gap (3.31 eV) and the highest aromaticity in double-ring clusters. This double-ring B_{14}^{2+} cluster is energetically lower than the quasi-planar one by even ~1.2 eV using high level *ab initio* calculations. B_{14}^{2+} also has 40 valence electrons as in Al_{13}^{-} cluster. The reason leading to the unusual properties of B_{14}^{2+} may be the electronic shell closing as in Al_{13}^{-} cluster based on the jellium model, besides the double aromaticity in all double-ring clusters. © *2012 American Institute of Physics*. [http://dx.doi.org/10.1063/1.4738957]

I. INTRODUCTION

Atomic boron is the first light element of group IIIA with one *p* valence electron. The short covalent radius, electron deficiency, large coordination number, and sp^2 hybridization of valence electrons allow boron to form strong directed chemical bonds with other atoms. As a result, boron can form diverse nanostructures, including quasi-planar, ring, nanotube, and cage structures.[1–15] At small cluster size, it is found that the planar or quasi-planar isomers are more stable than the three-dimensional (3D) ones.[1,2] The 2D to 3D (planar-to-tubular) structural transition occurs at B_{20}.[3] The neutral B_{20} was suggested to be a very stable double-ring structure with high symmetry and aromaticity.[4] The experimentally known B_{20} was found to possess very strong ring currents and there is a strong correlation between ring current strength and aromaticity.[16] Similarly, the double-ring B_{16}, B_{20}, and B_{24} are electronically closed-shell clusters.[16] For larger boron clusters, some tubular, cage, and core-shell structures are competitive.[5,14,17–21] This structural trend has been attributed to variations of aromatic characters. On one hand, the π systems of (quasi-)planar boron clusters are suggested to be delocalized and aromatic for some small clusters but to become localized with increasing cluster size.[2] On the other hand, the high aromaticity of a delocalized π system covering the inner and outer surfaces of the molecule may be beneficial to the stability of the double-ring B_{20}.[3,22] Very recently, we reported a novel lowest-energy cage structure for neutral B_{14} which undergoes a transition between 2D and 3D structures.[23]

In this article, we report an investigation of the "magic number" double-ring structure of B_{14}^{2+} cluster. This double-ring B_{14}^{2+} has a very large HOMO-LUMO (H-L) gap and high aromaticity, which is different from the other double-ring structures in many aspects.

II. COMPUTATIONAL METHODS

The TPSSh functional[24] is selected in density functional theory (DFT), which was proven to give reasonably accurate energetic properties of small boron clusters.[19,23] The low-lying isomers of B_{14}^{2+} cluster are found via two ways. One is to reoptimize the previously located[23] neutral B_{14} geometries at the TPSSh/6-311+G* level. The other is by unbiased global search of the DFT potential energy surface coupled with genetic algorithm directly using the TPSSh functional. In the global optimization procedure, we adopt a small basis set (3-21G) and a loose convergence criterion for saving calculation time. Then, we relax low-lying TPSSh/3-21G geometries fully at the TPSSh/6-311+G* level after global optimization. For further comparison, relative energies of the first two low-lying isomers at coupled-cluster single double triple (CCSD(T)) (Ref. 25)/aug-cc-pVTZ level of theory are given using the optimized geometries at the TPSSh/6-311+G* level. In the CCSD(T) calculations, only the valence electrons are correlated. Considering thermal corrections, free energies of the low-energy isomers of B_{14}^{2+} clusters are calculated at the TPSSh/6-311+G* level. The calculations of the HOMO-LUMO gaps, vibrational frequencies, and aromaticity are also performed at the TPSSh/6-311+G* level. All calculations are carried out using the GAUSSIAN 09 package.[26]

III. RESULTS AND DISCUSSION

The shapes, symmetry point groups, electronic states, and relative energies of the global minimum and low-energy isomers of B_{14}^{2+} are displayed in Fig. 1. The calculated vibrational frequencies of the low-energy isomers of B_{14}^{2+} clusters are verified to be all positive, so they are indeed local minima. The coordinates and vibrational frequencies of the low-energy isomers of B_{14}^{2+} clusters can be found in the supplementary material.[27] The global minimum (isomer **I**) is a double-ring structure in C_i symmetry. Jahn-Teller effects[28] slightly distort the double-ring structure from the ideal D_{7d} to C_i symmetry.[16,29] Isomer **II** is a quasi-planar structure in C_{2v} symmetry. Isomer **III** is a 3D structure in C_s symmetry. Isomer **IV** is a convex structure in C_{4v} symmetry. Isomer **V** is a quasi-planar structure in C_s symmetry. Isomer **VI** is a quasi-planar structure in C_{2v} symmetry. Isomer **VII** is a cage in D_{2d} symmetry, which is suggested to be a "magic number"

a)Author to whom correspondence should be addressed. Electronic mail: clj@ustc.edu. Tel./Fax: +86-551-5107342.

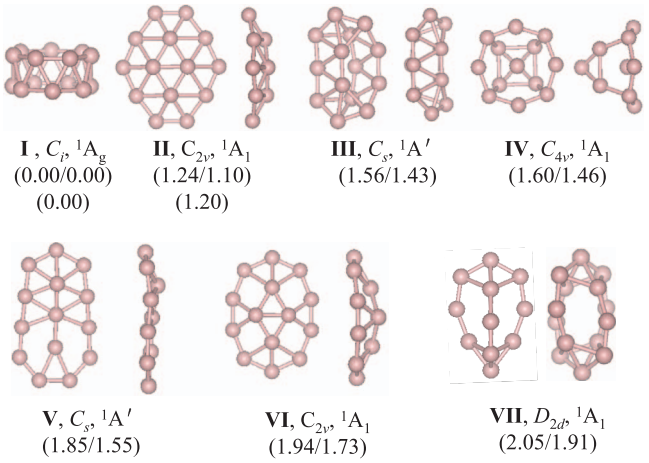

FIG. 1. Optimized geometry of the low-energy isomers (I-VII as labeled) of B_{14}^{2+} at TPSSh/6-311+G*. Symmetry and electronic state of each isomer are labeled, and enclosed are energies/free energies in eV relative to the first isomer at TPSSh/6-311+G*. For the first two isomers, relative energies at CCSD(T)/aug-cc-pVTZ are also labeled.

of neutral B_{14} cluster.[23] The structures of isomers **II**, **III**, **V**, **VI**, and **VII** are same with the ones of neutral B_{14} cluster.[23] Isomer **I** is more stable than isomer **II** by even 1.24 eV at TPSSh/6-311+G* level in agreement with the value (1.20 eV) at CCSD(T)/aug-cc-pVTZ level. And free energies are consistent with the energies without thermal corrections.

The double-ring B_{14}^{2+} is much lower than the quasi-planar one energetically, which is surprising at such a cluster size and so we suppose that it may be a "magic number" in electronic structure. For neutral clusters, a structural transition from 2D to 3D occurs at B_{20},[4] and the double-ring B_{20} is lower than the quasi-planar one by about 0.6 eV in energy at TPSSh/6-311+G* level. For cationic clusters, a structural transition from 2D to 3D occurs at B_{16}^+,[29] and the energy of double-ring B_{16}^+ is close to the one of quasi-planar B_{16}^+ at TPSSh/6-311+G* level. The double-ring B_{12}, B_{16}, B_{18}^{2-}, B_{18}^{2+}, and B_{20} are all doubly aromatic. Figure 2 plots the energies of the lowest-energy double-ring clusters relative to the lowest-energy quasi-planar ones at neutral B_{12}, B_{16}, and B_{20}, dication B_{14}^{2+} and B_{18}^{2+}, and dianion B_{18}^{2-}. From the figure, we can draw the following conclusions: (1) The relative stability of double-ring clusters, both neutral and charged, enhances with increasing cluster size; (2) The relative stability of double-ring clusters increases with more positive charge. The trends of the relative stability with the size and charge are labeled in Fig. 2. In a word, the relative stability of double-ring clusters depends on the size and the charge state of the clusters. However, the B_{14}^{2+} cluster is anomalous according to the above rules. The double-ring structure is unusually more stable than the quasi-planar one in B_{14}^{2+} cluster, which hints a "magic number" in the doubly aromatic double-ring clusters.

Next, we show the H-L gaps and the nucleus-independent chemical shifts (NICS) values (at the center) of the global minimum quasi-planar B_{12} and cage B_{14} and the lowest-energy double-ring B_{12}, B_{14}^{2+}, B_{16}, B_{18}^{2-}, B_{18}^{2+}, and B_{20} in Table I. NICS value[30] is the most widely used as a quantitative measure for aromaticity (negative NICS values mean

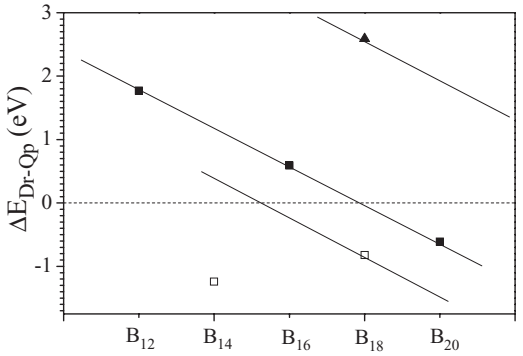

FIG. 2. Energies of the lowest-energy double ring clusters relative to the lowest-energy quasi-planar ones ($\Delta E_{Dr\text{-}Qp}$) at neutral (filled square) B_{12}, B_{16}, and B_{20}, dication (square) B_{14}^{2+} and B_{18}^{2+}, and dianion (filled triangle) B_{18}^{2-}.

aromaticity and positive NICS values mean anti-aromaticity). As shown in Table I, the double-ring B_{14}^{2+} has the largest HOMO-LUMO gap with 3.31 eV in the double-ring clusters and even larger than the "magic number" quasi-planar B_{12} (3.01 eV) and cage B_{14} (2.69 eV). Additionally, according to the NICS values, the double-ring B_{14}^{2+} is most aromatic (−44.14 ppm) in the double-ring clusters, and is very close to the B_{14} cage (−44.23 ppm) which is an all-boron fullerene with 18 delocalized electrons in the highest spherical aromaticity.[31] As a result, the double-ring B_{14}^{2+} is suggested to be more stable in electronic structure and more aromatic than the known most aromatic double-ring B_{20}, which indicates a "magic number" in double-ring clusters.

Why is this double-ring structure unusually stable? First, we focus on the bonding nature in this structure. B_{14}^{2+} has a D_{7d}/C_i ground state double-ring geometry. The B–B bond lengths within the B_7 rings are 1.62 Å, and those connecting the two rings are 1.72 Å. Note that the B–B single bond distance is about 1.73 Å and B=B double-bond lengths experimentally characterized vary between 1.57 and 1.59 Å.[22,32–34] According to the distribution of bond lengths above, we suggest that there must be strong delocalization of electrons within and between the rings.

In order to gain insight into the nature of the bonding in the double-ring B_{14}^{2+}, we carried out canonical molecular orbital (MO) analysis. Note that B_{14}^{2+} has 40 valence electrons. Figures 3(a) and 3(b) depict the 20 MOs (MO = 15–34) of va-

TABLE I. The HOMO-LUMO gaps (H-L) and NICS values (at the center) of the global minimum B_{12} and B_{14} and the lowest-energy double-ring B_{12}, B_{14}^{2+}, B_{16}, B_{18}^{2-}, B_{18}^{2+}, and B_{20}.

Species	Motif	Point group	H-L (eV)	NICS(0) (ppm)
B_{12}	Quasi-planar	C_{3v}	3.01	−28.36
B_{14}	Cage	D_{2d}	2.69	−44.23
B_{12}	Double ring	D_{2d}	2.38	−31.77
B_{14}^{2+}	Double ring	C_i	3.31	−44.14
B_{16}	Double ring	C_{4v}	1.86	−30.87
B_{18}^{2-}	Double ring	C_i	1.18	−37.29
B_{18}^{2+}	Double ring	C_{2h}	1.50	−27.85
B_{20}	Double ring	D_{2d}	2.05	−39.54

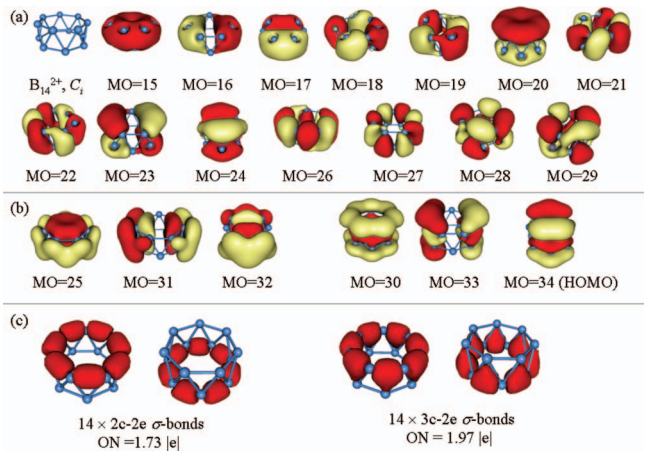

FIG. 3. (a) and (b) Structure and canonical MOs of the B_{14}^{2+} (C_i) cluster; (c) Results of the AdNDP localization (molecular visualization was performed using MOLEKEL 5.4).

lence electrons. From the MOs diagrams, we can identify the delocalized orbitals easily (MO = 25, 30–34 in Fig. 3(b)), including three radial and three tangential orbitals in tensor surface harmonic theory of cluster bonding[35–37] that are similar to the double-ring B_{12} cluster.[38] For example, the double-ring B_{12} (D_{6d}) has 6 tangential and 6 radial electrons achieving a $4n+2$ count in each of the tangential and radial subsystems, which is double-aromatic; the double-ring B_{14} (C_1) has 6 tangential and 8 radial electrons, which is tangential-aromatic and radial-antiaromatic; the double-ring B_{16} (D_{8d}) has 6 tangential and 10 radial electrons, which is double-aromatic; B_{18} has 8 tangential and 10 radial electrons, which is tangential-antiaromatic and radial-aromatic; B_{20} has 10 tangential and 10 radial electrons, which is double-aromatic. Similarly, the double-ring B_{14}^{2+} with 6 radial and 6 tangential electrons is double-aromatic consisted of both radial and tangential Hückel's aromaticity, which is consistent with the above-mentioned double-aromatic double rings. The remaining 14 pairs of valence electrons are localized on 14 B–B σ-bonds. However, there is some dispute about the B–B σ-bonds (2c–2e or 3c–2e) of the double-ring structure.[38,39] Usually, two patterns of covalent bonds are disputed: one pattern of two-center bonds in each ring and another one of three-center trilaterally formed bonds between two rings. For the purpose of settling this dispute, we apply a new tool named adaptive natural density partitioning (AdNDP) to obtain patterns of chemical bonding. The method was recently developed by Zubarev and Boldyrev.[40,41] AdNDP is based on the concept of the electron pair as the main element of chemical bonding models, which recovers both Lewis bonding elements (1c–2e and 2c–2e objects) and delocalized bonding elements (nc–2e).

According to the results of AdNDP analysis, two patterns of B–B bonding frameworks are displayed in Fig. 3(c): fourteen 2c–2e B–B σ-bonds with occupation numbers ON = 1.73 |e| and fourteen 3c–2e B–B σ-bonds with ON = 1.97 |e|. In the former pattern, the 2c–2e σ-bonds are equivalent and each boron atom contributes about 0.87 |e| equally. The latter pattern (3c–2e) is based on 2c–2e σ-bonds, but the 3c–2e σ-bonds are extremely inequivalent, and the third boron atom at the vertex of a triangle contributes only 0.24 |e| (1.97–1.73). So the B–B bonding of the double-ring B_{14}^{2+} is between Lewis bonding and delocalized σ-bonding. If the remaining 14 pairs of valence electrons are suggested to be involved in fourteen 3c–2e B–B σ-bonds, the 40 valence electrons of B_{14}^{2+} should be delocalized as in Al_{13}^- cluster.[42] The double-ring B_{14}^{2+} can also be taken as a 3D structure, which may be in electronic shell closing as in Al_{13}^- cluster based on the jellium model.[43–45] Jellium model[46] is often used as a simple model of delocalized electrons in metal clusters, in which all valence electrons are delocalized in the cluster volume and fill discrete energy levels.

To verify the effect of jellium model, we compare the aromaticity of double-ring B_{14}^{2+} with spherical aromatic C_{20}^{2+} and current aromatic B_{20}. Spherical aromaticity[31,47] arises from the π-electron system and follows the $2(n+1)^2$ rule, i.e., C_{20}^{2+} ($n = 2$) and C_{60}^{10+} ($n = 4$) are spherical aromatic, and it decays fast. The π-electron system of an icosahedral fullerene can be considered approximately as a spherical electron gas, which surrounds the surfaces of a sphere in a double skin. Current aromaticity[47] is induced by diamagnetic ring currents and follows the Hückel rule, i.e., benzene and annulenes with $4n+2$ π electrons are current aromatic, and it decays more slowly than spherical aromatic. Note that the cage C_{20}^{2+} is an icosahedral fullerene satisfying the $2(n+1)^2$ rule for spherical aromaticity ($n = 2$),[31,48] in which spherical aromaticity decays rapidly. The aromaticity of the double-ring B_{20} is induced by diamagnetic ring currents,[16] in which the aromaticity decays more slowly than spherical aromaticity. In terms of aromaticity, we suspect that the decaying speed of the double-ring B_{14}^{2+} may be between the one of the cage C_{20}^{2+} and the one of the double-ring B_{20}. In order to confirm this supposition, Fig. 4 plots the NICSzz-scan curves for the double-ring B_{14}^{2+}, B_{20}, and the cage C_{20}^{2+} within the range of 0.0–8.0 Å above the geometric centers of the systems. The NICSzz-scan is similar to the aromatic ring current shieldings approach,[49] which can provide a clear picture of the type of the ring current in aromatic and antiaromatic systems[50,51] and can be used to characterize whether an inorganic system is aromatic, nonaromatic, and antiaromatic.[52,53] From Figure 4, we found that

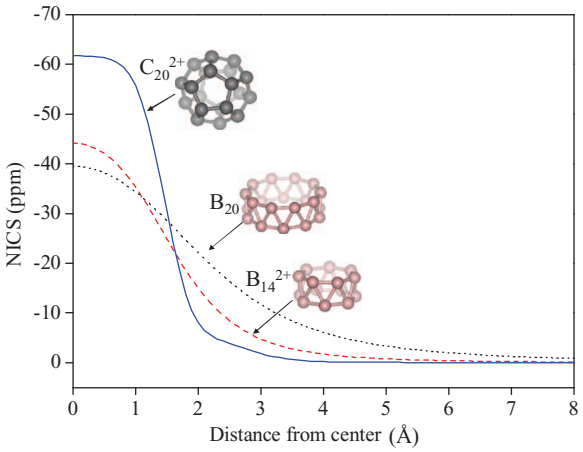

FIG. 4. The NICSzz-scan curves for B_{20} (dotted line), B_{14}^{2+} (dashed line), and C_{20}^{2+} (solid line), within the range of 0.0–8.0 Å above the geometric centers of the systems.

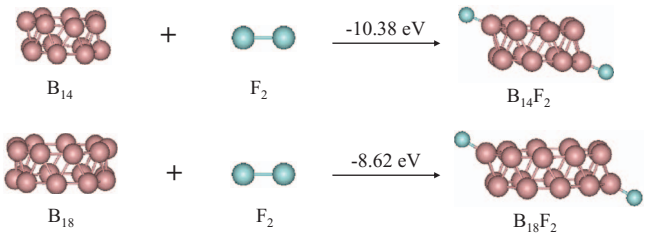

FIG. 5. Formation of $B_{14}F_2$ ($B_{18}F_2$) from neutral double-ring B_{14} (B_{18}) cluster and F_2 at TPSSh/6-311+G*. Reaction enthalpies (eV) are labeled.

NICS value of the double-ring B_{14}^{2+} decays more slowly than the one of the cage C_{20}^{2+}, faster than the one of the double-ring B_{20}. That is, the aromaticity of the double-ring B_{14}^{2+} is between spherical and current aromaticity, which is in agreement with our prediction. Thus, the effect of jellium model may exist in the double-ring B_{14}^{2+} cluster.

For the dication B_{14}^{2+} molecule, reaction energies cannot be achieved. To further prove the effect of jellium model, the enthalpies of formation of $B_{14}F_2$ and $B_{18}F_2$ from neutral double-ring B_{14} (B_{18}) cluster and F_2 are compared and the results are shown in Fig. 5. The $B_{14}F_2$ is stable and the enthalpy is -10.38 eV (for comparison, the enthalpy of formation of HF from H_2 and F_2 is -5.47 eV), which still keeps the double-ring structure with a large HOMO-LUMO gap (2.79 eV) and high aromaticity (NICS(0) $= -37.76$ ppm). The electronic structure of $B_{14}F_2$ is similar to the one of the dication double-ring B_{14}^{2+}. However, the enthalpy of formation of the $B_{18}F_2$ (-8.62 eV) is smaller than the one of $B_{14}F_2$ by about 1.76 eV. $B_{18}F_2$ also keeps the double-ring structure, but the HOMO-LUMO gap of $B_{18}F_2$ (1.47 eV) is also smaller than the one of $B_{14}F_2$. The above analysis suggests that neutral B_{14} cluster is unstable and tends to lose two electrons. In $B_{14}F_2$ cluster, two extra electrons of neutral B_{14} are mostly localized on two B–F bonds, which further prove that the 40 delocalized valence electrons of B_{14}^{2+} fill electronic shells as in Al_{13}^- cluster based on the jellium model and the effect of jellium model also may make the enthalpy of formation of $B_{14}F_2$ cluster lower.

Briefly, the reasons leading to the unusual properties of the double-ring B_{14}^{2+} may be the effect of jellium model besides the radial and tangential Hückel's aromaticity. The unusual aromaticity and the lower enthalpy of formation of $B_{14}F_2$ also may due to the effect of jellium model, but the effect of jellium model is not as strong as the one in metallic clusters. $B_{14}F_2$ is more stable than $B_{18}F_2$ by 1.76 eV reference to neutral boron cluster and F_2 molecule. Thus, the contribution of jellium effect in B_{14}^{2+} clusters is also about 1.76 eV, and the double-ring B_{14}^{2+} clusters will be about 0.5 eV higher in energy than the quasi-planar one without jellium effect.

IV. CONCLUSIONS

In conclusion, we report an unusual double-ring structure of B_{14}^{2+} cluster. The double-ring B_{14}^{2+} has a very large HOMO-LUMO gap and is more aromatic than the known most aromatic double-ring B_{20}, which suggests that it is a "magic number" in the double-ring clusters. The canonical MOs analysis reveals that it is doubly aromatic and the AdNDP analysis indicates that B–B bonding of the double-ring B_{14}^{2+} is between Lewis bonding and delocalized σ-bonding. The 40 delocalized valence electrons of B_{14}^{2+} fill electronic shells as in Al_{13}^- cluster based on the jellium model. The effect of jellium model is found first in a non-metallic cluster, although the evidence is indirect and the effect is small. The lower enthalpy of formation of $B_{14}F_2$ also provides an indirect proof for that B_{14}^{2+} may be the electronic shell closing as in Al_{13}^- cluster based on the jellium model. The reasons for the unusual properties of the double-ring B_{14}^{2+} may be radial and tangential Hückel's aromaticity and the effect of jellium model.

ACKNOWLEDGMENTS

It is a pleasure to thank Professor Boldyrev for the AdNDP codes. This work is supported by the National Natural Science Foundation of China (NNSFC) (20903001), by the 211 Project and the Outstanding Youth Foundation of Anhui University. The calculations are carried out on the High-Performance Computing Center of Anhui University.

[1] I. Boustani, Phys. Rev. B **55**, 16426 (1997).
[2] H. J. Zhai, B. Kiran, J. Li, and L. S. Wang, Nat. Mater. **2**, 827 (2003).
[3] W. An, S. Bulusu, Y. Gao, and X. C. Zeng, J. Chem. Phys. **124**, 154310 (2006).
[4] B. Kiran, S. Bulusu, H. J. Zhai, S. Yoo, X. C. Zeng, and L. S. Wang, Proc. Natl. Acad. Sci. U.S.A. **102**, 961 (2005).
[5] F. Y. Tian and Y. X. Wang, J. Chem. Phys. **129**, 24903 (2008).
[6] D. Ciuparu, R. F. Klie, Y. Zhu, and L. Pfefferle, J. Phys. Chem. B **108**, 3967 (2004).
[7] S. J. Xu, J. M. Nilles, D. Radisic, W. J. Zheng, S. Stokes, K. H. Bowen, R. C. Becker, and I. Boustani, Chem. Phys. Lett. **379**, 282 (2003).
[8] A. Quandt and I. Boustani, Chem. Phys. Chem. **6**, 2001 (2005).
[9] I. Boustani, A. Quandt, E. Hernandez, and A. Rubio, J. Chem. Phys. **110**, 3176 (1999).
[10] M. A. L. Marques and S. Botti, J. Chem. Phys. **123**, 014310 (2005).
[11] S. Chacko, D. G. Kanhere, and I. Boustani, Phys. Rev. B **68**, 035414 (2003).
[12] K. C. Lau, M. Deshpande, R. Pati, and R. Pandey, Int. J. Quantum Chem. **103**, 866 (2005).
[13] I. Boustani, A. Rubio, and J. A. Alonso, Chem. Phys. Lett. **311**, 21 (1999).
[14] N. G. Szwacki, A. Sadrzadeh, and B. I. Yakobson, Phys. Rev. Lett. **98**, 166804 (2007).
[15] Z. A. Piazza, W. L. Li, C. Romanescu, A. P. Sergeeva, L. S. Wang, and A. I. Boldyrev, J. Chem. Phys. **136**, 10 (2012).
[16] M. P. Johansson, J. Phys. Chem. C **113**, 524 (2009).
[17] L. Wang, J. J. Zhao, F. Y. Li, and Z. F. Chen, Chem. Phys. Lett. **501**, 16 (2010).
[18] C. Özdoğan, S. Mukhopadhyay, W. Hayami, Z. B. Güvence, and I. Boustani, J. Phys. Chem. C **114**, 4362 (2010).
[19] J. J. Zhao, L. Wang, F. Y. Li, and Z. F. Chen, J. Phys. Chem. A **114**, 9969 (2010).
[20] B. Shang, L. F. Yuan, X. C. Zeng, and J. L. Yang, J. Phys. Chem. A **114**, 2245 (2010).
[21] H. Li, N. Shao, B. Shang, L. F. Yuan, J. L. Yang, and X. C. Zeng, Chem. Commun. **46**, 3878 (2010).
[22] B. Kiran, G. Kumar, M. T. Nguyen, A. K. Kandalam, and P. Jena, Inorg. Chem. **48**, 9965 (2009).
[23] L. J. Cheng, J. Chem. Phys. **136**, 104301 (2012).
[24] T. Tao, J. P. Perdew, V. N. Staroverov, and G. E. Scuseria, Phys. Rev. Lett. **91**, 146401 (2003).
[25] A. D. Becke, Phys. Rev. A **38**, 3098 (1988).
[26] M. J. Frisch, G. W. Trucks, H. B. Schlegel *et al.*, GAUSSIAN 09, Revision B.01, Gaussian, Inc., Wallingford, CT, 2009.
[27] See supplementary material at http://dx.doi.org/10.1063/1.4738957 for the coordinates and vibrational frequencies of the low-energy isomers of B_{14}^{2+} clusters.

[28]R. Englman and J. Birks, *The Jahn-Teller Effect in Molecules and Crystals* (Wiley-Interscience, New York, 1972), p. 350.
[29]E. Oger, N. R. M. Crawford, R. Kelting, P. Weis, M. M. Kappes, and R. Ahlrichs, Angew. Chem., Int. Ed. **46**, 8503 (2007).
[30]P. von R. Schleyer, C. Maerker, A. Dransfeld, H. Jiao, and N. J. R. van Eikema Hommes, J. Am. Chem. Soc. **118**, 6317 (1996).
[31]Z. Chen, H. Jiao, A. Hirsch, and W. Thiel, J. Mol. Model. **7**, 161 (2001).
[32]A. A. Korkin, P. R. Schleyer, and M. L. McKee, Inorg. Chem. **34**, 961 (1995).
[33]A. Moezzi, M. M. Olmstead, and P. P. Power, J. Am. Chem. Soc. **114**, 2715 (1992).
[34]A. Moezzi, R. A. Barlett, and P. P. Power, Angew. Chem., Int. Ed. Engl. **31**, 1082 (1992).
[35]A. J. Stone, Mol. Phys. **41**, 1339 (1980).
[36]A. J. Stone, Inorg. Chem. **20**, 563 (1981).
[37]A. J. Stone and M. J. Alderton, Inorg. Chem. **21**, 2297 (1982).
[38]D. E. Bean and P. W. Fowler, J. Phys. Chem. C **113**, 15569 (2009).
[39]H. Tang and S. Ismail-Beigi, Phys. Rev. Lett. **99**, 115501 (2007).
[40]D. Yu. Zubarev and A. I. Boldyrev, Phys. Chem. Chem. Phys. **10**, 5207 (2008).
[41]D. Y. Zubarev and A. I. Boldyrev, J. Org. Chem. **73**, 9251 (2008).
[42]D. E. Bergeron, A. W. Castleman, Jr., T. Morisato, and S. N. Khanna, Science **304**, 84 (2004).
[43]S. Burkart, N. Blessing, B. Klipp, J. Müller, G. Ganteför, and G. Seifert, Chem. Phys. Lett. **301**, 546 (1999).
[44]C. Ashman, S. Khanna, and M. Pederson, Phys. Rev. B **66**, 193408 (2002).
[45]A. Castleman, Jr. and S. Khanna, J. Phys. Chem. C **113**, 2664 (2009).
[46]M. Brack, Rev. Mod. Phys. **65**, 677 (1993).
[47]A. Hirsch, Z. Chen, and H. Jiao, Angew. Chem., Int. Ed. **39**, 3915 (2000).
[48]A. Hirsch, Z. Chen, and H. Jiao, Angew. Chem., Int. Ed. **40**, 2834 (2001).
[49]J. Juselius and D. Sundholm, Phys. Chem. Chem. Phys. **1**, 3429 (1999).
[50]A. Stanger, J. Org. Chem. **71**, 883 (2006).
[51]A. Stanger, Chem. Eur. J. **12**, 2745 (2006).
[52]J. Poater, J. M. Bofill, P. Alemany, and M. Solà, J. Org. Chem. **71**, 1700 (2006).
[53]J. O. C. Jiménez-Halla, E. Matito, J. Robles, and M. Solà, J. Organomet. Chem. **691**, 4359 (2006).